Title
Trends and Control in the Nitridation of Transition-Metal Surfaces

Journal
ACS Catalysis, 8(1)

ISSN
2155-5435

Authors
Wang, Tao
Yan, Zhen
Michel, Carine
et al.

Publication Date
2018-01-05

DOI
10.1021/acscatal.7b02096

Peer reviewed

Trends and Control in the Nitridation of Transition Metal Surfaces

Tao Wang,[a] Zhen Yan,[b] Carine Michel,[a] Marc Pera-Titus,[b] Philippe Sautet*[a,c]

a) Univ Lyon, ENS de Lyon, CNRS UMR 5182, Université Claude Bernard Lyon 1, Laboratoire de Chimie, F69342, Lyon, France.

b) Eco-Efficient Products and Processes Laboratory (E2P2L), UMI 3464 CNRS-Solvay, 3966 Jin Du Road, Xin Zhuang Industrial Zone, 201108 Shanghai, China.

c) Department of Chemical and Biomolecular Engineering, University of California, Los Angeles, Los Angeles, CA 90095, United States.

E-mail: sautet@ucla.edu

Abstract: Understanding and predicting the nature of transition metal surfaces under realistic pressure and temperature conditions is crucial for optimizing their catalytic, mechanical or electronic properties. We focus here on the stability of transition metal surfaces submitted to a pressure of NH_3 and H_2 and on the potential formation of metastable or stable surface nitrides. Our leading example is a Ni-based alcohol amination catalyst, studied by a combination of DFT, thermodynamic modeling and experiments. Initial N-coverage on Ni nanoparticles selectively occurs on (100) facets, which become the most stable termination. Concomitantly, the equilibrium shape of the particle becomes modified under a realistic gas-phase environment of NH_3 and H_2. Extreme conditions favor the genesis of a metastable Ni_3N nanoparticles, mainly exposing (101) termination. Transformation into Ni and gas-phase N_2, favored by thermodynamics, is kinetically hindered. H_2 controls the catalyst nitridation by the competition between H-covered and N-covered surfaces. Extension to fifteen transition metals unveils a huge spectrum of nitridation behaviors arising from very reactive Mo to almost inert Au. Nonetheless, in several cases, a moderate H_2 pressure is sufficient to prevent nitridation under a pressure of NH_3. The approach presented in this study gives insight into the surface nitridation behavior of transition metals, paving the way to *in silico* design under real conditions for applications in Materials Science and Heterogeneous Catalysis.

Keywords: Catalysis, DFT, Thermodynamics, Amination, Nitridation

Introduction

Nitridation of transition metals and oxides with NH_3 is a well-known process that can be used in Materials Science for generating phases with useful optical, electronic, magnetic and mechanical superhard properties.[1,3] For example, the synthesis of binary transition metal nitrides as protective layers is the basic step in the industrial steel surface hardening process.[4] In the case of noble metal nitrides, each successful synthesis has always been regarded as a breakthrough in the field.[1,2] A decade ago, Gregoryanz *et al*.[5] reported the first discovery and characterization of binary platinum nitride (PtN), which is stable even at room temperature and ambient pressure. Using a similar method but at higher temperatures and pressures, the synthesis of iridium,[6] palladium,[7] osmium[8] and rhenium[9] nitrides was also succeeded. This work was essentially motivated by the quest of superhard materials generated by the combination of light elements such as nitrogen or boron with transition metals that have high elastic moduli on the guidance of the proposal by Kaner *et al*.[10]

In heterogeneous catalysis, nitridation can result in two different scenarios depending on the metal. On the one hand, transition metal nitrides such as Mo_2N and W_2N are widely used in hydrotreatment reactions and their activities are comparable to those commonly attained on noble metal catalysts.[11,12] Mo_2N and Mo_3Co_3N are also well-known catalysts for N_2 activation in the synthesis of NH_3.[13] Furthermore, nitride Ni_3N nanosheet has been reported as an efficient and inexpensive catalyst for the oxygen evolution reaction (OER).[14] The formation of surface N-H species over supported Ni upon exposure to a low-partial pressure of NH_3 (500 ppm) is also known to promote the partial hydrogenation of 1,3-butadiene to 1-butene in the temperature range 303-373 K.[15]

On the other hand, transition metal nitridation during reaction can act as a catalyst deactivation pathway and should therefore be avoided. A paradigmatic example of this latter situation can be found in the direct amination of alcohols with NH_3 and amines over metal catalysts. This reaction is attractive, since water is obtained as main byproduct and alcohols issued from biomass resources in biorefineries can be directly implemented to synthesize amines.[16] The most studied heterogeneous catalysts for the synthesis of aliphatic amines comprise Ni,[17] Cu,[18] NiCu,[19] and Co[20] nanoparticles over alkaline or amphoteric oxides (*e.g.*, γ,θ-Al_2O_3). These catalysts are known to suffer from deactivation during the reaction due to the formation of surface nitrides by ammonolysis of the metal in the presence of NH_3.[21] In practice, even if alcohol amination does not require *per se* H_2 as a reactant, a H_2 pressure is required to mitigate the formation of surface nitrides and prevent N-incorporation into the metal lattice. Metal nitrides are also known to catalyze unwanted side reactions such as alcohol dehydration, deamination of amines into olefins and amine disproportionation into more substituted amines, impacting on the selectivity of the amination reaction.[22] Hence understanding and controlling catalyst nitridation has strong potential impact in the performance of heterogeneous catalysis for amination reactions either to decrease the required H_2 pressure, or to improve the selectivity.

Surface and bulk nitridation processes open key questions in Materials Science and Heterogeneous Catalysis: (1) What is the most stable phase, metal or nitride, as a function of the working conditions? (2) Which metals are more prone to surface or bulk nitridation? (3) How does the shape of nanoparticles evolve under reaction conditions? (4) How to avoid or slow down nitridation and hence catalyst deactivation in direct amination reactions? By combining DFT calculations, thermodynamic modelling and experiments, here we devise general trends of surface and bulk nitridation of transition metals to gain insights into the factors and conditions controlling this transformation.

Method Section

All computations were performed by applying the Density Functional Theory (DFT) method using the Vienna *Ab Initio* Simulation Package (VASP).[23] The electron-ion interaction was described with the projector augmented wave (PAW) method,[24] while the electron exchange and correlation energy was solved within the generalized gradient approximation under the Perdew-Burke-Ernzerhof formalism (GGA-PBE).[25] An energy cut-off of 400 eV was used to ensure accurate energies. Convergence of N-adsorption energies with slab thickness was carefully verified (SI, Table S3). Additional details on the DFT and thermodynamic methods are given in SI.

The Ni nitridation experiments were conducted at ambient pressure over NiO nanoparticles previously reduced at 573 K for 30 min under 10% H_2/He flow (average particle size of 84 nm). Three series of experiments were carried out at 473 K for 3 h: (1) nitridation in the presence of 10%NH_3 / 90%He; (2) nitridation in the presence of 5%NH_3, 5%H_2 and balance He; and (3) hydrogenation at 473 K for 3 h after nitridation using a 10%H_2 / 90%He flow. After nitridation, the temperature-programmed desorption profiles were measured from room temperature to 1073 K under He using a 10 K/min heating ramp. More details on the different protocols can be found in the SI.

Results and discussions

To answer the different questions, our choice was first oriented to Ni exposed to a pressure of NH_3 and H_2 at representative conditions of amination reactions. Three possible phases were considered, namely metallic Ni, N-covered Ni surface and Ni nitride in the most stable hcp Ni_3N phase. When comparing these three phases, the N chemical potential (μ_N) appears as a key variable. For bulk structures, Ni metal is more stable for μ_N lower than -8.2 eV, while the bulk nitride is favored at higher chemical potential. Let us now discuss the most stable surface structure and the equilibrium shape for a nanoparticle for each phase separately. For bare Ni, seven surfaces are exposed on the optimum Wulff shape, where Ni(111) surface takes the highest proportion (62%), followed by Ni(100) (17.5%), while the other five surfaces are present at a proportion lower than 10% (see leftmost particle shape in Figure 1, Table S1 and Figure S1-S2).

These seven terminations of Ni exhibited a variable interaction with N atoms (represented in Figure S3). Based on the average adsorption energy (Table S3), it is found that the saturation coverage is 2/3 monolayer (ML), 1 ML, 1/3 ML, 7/4 ML, 3/4 ML, 1 ML and 5/6 ML on the Ni(100), (110), (111), (210), (211), (221) and (311) surfaces, respectively. Among these surfaces, Ni(100) and (210) surfaces show the strongest N adsorption, which indicates a higher capacity for being nitridated. Based on these extensive DFT calculations, a thermodynamic model was applied to determine the most stable coverage by N atoms on each surface as a function of μ_N (Figure S4-S5, Table S4)[26] At low μ_N, nitrogen does not adsorb on Ni. The onset chemical potential is at μ_N =-9.2 eV, where the (100) surface starts to be N-covered and is progressively stabilized, becoming more stable than the bare Ni(111) at μ_N =-8.7 eV, with a N-coverage of 1/3 ML (Figure 1). Although other surfaces start to be N-populated at higher μ_N (-8.6 eV and -8.5 eV for Ni(110) and Ni(111), respectively), Ni(100) remains the most stable surface in the μ_N range explored, with a higher N-coverage while increasing μ_N. Note however that, as stated earlier, bulk Ni_3N becomes more stable than metal Ni bulk above -8.2 eV, and the different N-Ni surface systems become metastable.

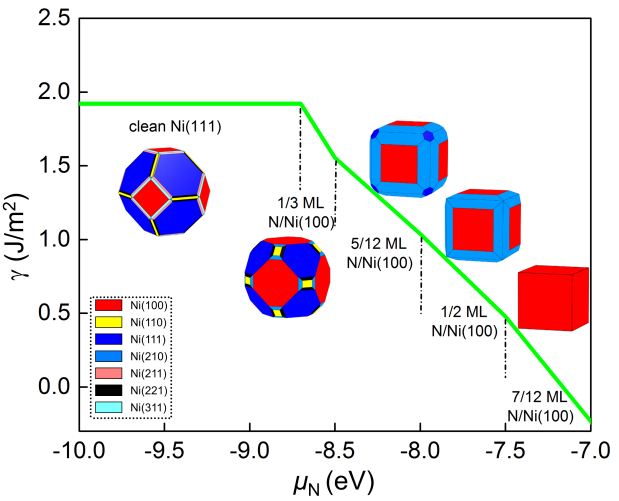

Figure 1. Surface energies (γ) of the most stable termination of metallic Ni as a function of the nitrogen chemical potential (μ_N). Seven bare or N covered Ni surfaces have been considered. The optimal Wulff shape of a Ni particle is given for μ_N = -9.5, -8.75, -8.25, -7.75 and -7.25 eV, respectively.

The typical shape of Ni nanoparticles is also expected to suffer from severe morphological changes upon nitridation. At low μ_N, Ni(111) terraces dominate, whereas the N-covered Ni(100) termination gradually takes over at higher μ_N, which is accompanied by the stepped (210) surface (Figure 1). Hence, a strong restructuration of the Ni nanoparticle is expected to occur due to preferential N-adsorption on the Ni(100) termination, resulting in its complete deactivation.

Let us now turn our attention into the Ni nitride phase (Ni_3N), which becomes stable against Ni bulk at a μ_N higher than -8.2 eV. The low-miller index (001), (100), (101), (110) and (111) surfaces with 26 different terminations for the truncation and at variable N-coverage were chosen as models and detailed structural information is provided in the SI (Figure S6 and Table S4).

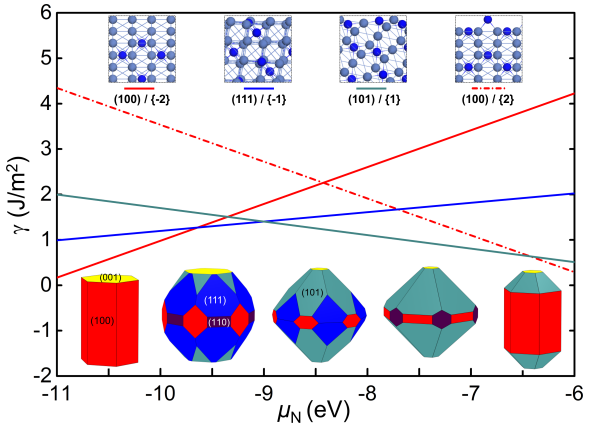

Figure 2. Surface energies (γ) of the most stable terminations for Ni_3N as a function of the nitrogen chemical potential (μ_N). The most stable termination corresponds to the lowest surface energy ((100) in red, (111) in blue and (101) in grey, (100) / {-2} means a 2 less N from Ni_3N stoichiometry per surface Ni atom of (100) termination. Relevant morphologies for the Ni_3N nanoparticles from Wulff construction are shown for μ_N = -10.5, -9.5, -8.5, 7.5 eV and -6.0 eV.

Figure 2 compiles the surface energies (γ) for the most stable Ni_3N terminations (referred to as bulk Ni_3N) as a function of μ_N (a complete diagram is provided in Figure S7). The slope of γ as a function of μ_N is, by definition, related to the stoichiometry of the termination: N-deficient terminations exhibit a positive slope, while N-rich terminations show a negative slope.[26] N-deficient terminations become more stable at lower μ_N, whereas N-rich terminations display the opposite trend. For example, with μ_N < -9.6 eV, the Ni-rich (100)/{-2} termination is the most stable; at -9.6 eV < μ_N < -9.0 eV, the (111)/{-1} termination becomes the most stable; at -9.0 eV < μ_N < -6.5 eV, the (101)/{1} termination is the most stable; and at μ_N > -6.5 eV, the N-rich (100)/{2} termination becomes the most stable. The different stability orders for each surface results ultimately in a different Ni_3N morphology at a given μ_N, which could be clearly revealed by corresponding Wulff shapes. Considering the stability region of the bulk nitride at μ_N>-8.2 eV, the N rich (101) termination becomes the most stable and hence exposed surface for Ni_3N.

With this information in hand for the metallic Ni and Ni_3N phases separately, we can now discuss more specifically the surface stability of Ni in the conditions of amination reactions. Figure 3 depicts two versions of the surface stability diagram for Ni as a function of the N (μ_N) and H chemical potential (μ_H) (Figure 3a), and as a function of the temperature and H_2 partial pressure for an NH_3 partial pressure of 101 kPa (Figure 3b). Note that the partial pressure of both NH_3 and H_2 need to be specified to determine μ_N. In these plots, the formation energies of Ni slabs, Ni slabs covered by N, H, N+H, NH_3, NH_3+H and Ni_3N slabs with variable surface N content are compared. A constrained equilibrium was explored, where N_2 formation is excluded. Indeed, N_2 desorption from Ni is associated to a high barrier (>1.7 eV) and a long reaction time (2500 h at 450 K).[27] In contrast, NH_3 dissociation is much faster, with a barrier of 1 eV on Ni(211).[28] In Figure 3, NH_3 dissociation is allowed for the optimum surface determination, while N_2 dissociation is forbidden.

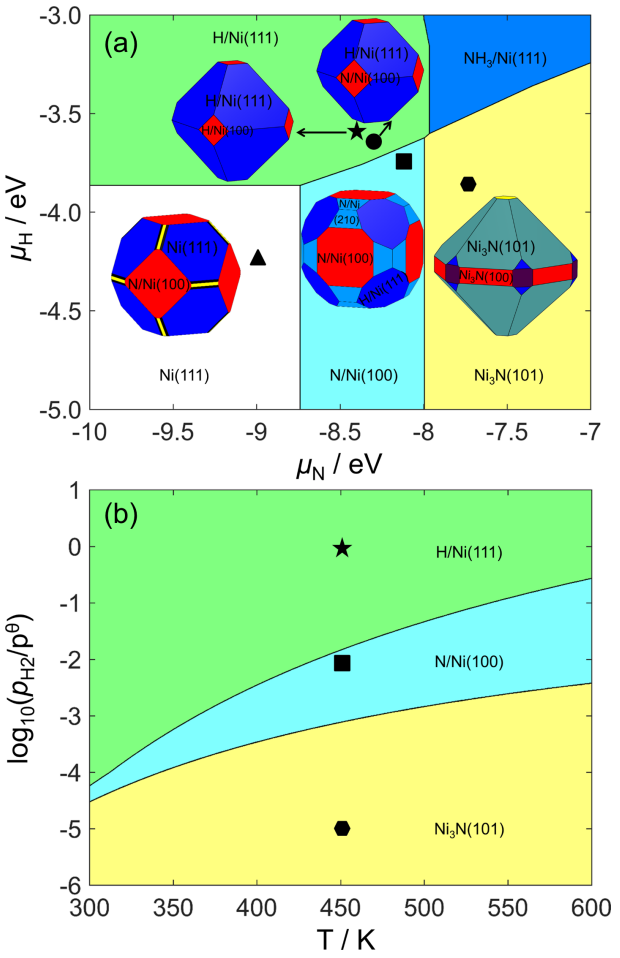

Figure 3. (a) Most stable phase and surfaces for Ni using Wulff constructions as a function of the nitrogen (μ_N) and hydrogen (μ_H) chemical potentials, and (b) most stable phase and most stable surface as a function of the temperature and the H_2 partial pressure at p_{NH3} = 101 kPa. Specific conditions are indicated as follows: black dot (T = 450 K, p_{NH3} = 66.7 kPa, p_{H2} = 18.5 kPa, i.e., μ_N = -8.30 eV and μ_H = -3.64 eV); black star (T = 450 K, p_{NH3} = p_{H2} = 101 kPa, i.e., μ_N = -8.38 eV and μ_H = -3.61 eV); black square (T = 450 K, p_{NH3} = 101 kPa, p_{H2} = 1 kPa, i.e., μ_N = -8.12 eV and μ_H = -3.70 eV), black hexagon (T = 450 K, p_{NH3} = 101 kPa and p_{H2} = 10^{-3} kPa, i.e., μ_N = -7.71 eV and μ_H = -3.83 eV), and black triangle (T = 450 K, p_{N2} = p_{H2} = 10^{-12} kPa, i.e., μ_N = -9.00 eV and μ_H = -4.24 eV).

To start, it is worth noting that the bare Ni surface is never the most stable one in the presence of a pressure of NH_3 of 101 kPa. At high H_2 pressure (i.e. high H chemical potential), the most stable termination is H-covered Ni(111) and nitridation is unlikely. Typical reaction conditions for alcohol amination (p_{NH3} = 66.7 kPa and p_{H2} = 18.5 kPa and T = 450 K, black dot in Figure 3a) correspond to this case and Ni nanoparticles expose primarily the H-covered (111) surface and to a minor extent the N-covered (100) surface. Switching to standard pressures (p_{NH3} = p_{H2} = 101 kPa; black star in Figure 3) mainly increases the H_2 partial pressure and the Ni nanoparticles are expected to expose preferentially H-covered Ni(111) and (100) surfaces. If the H_2 partial pressure

is reduced to 1 kPa at 450 K (black square in Figure 3), μ_H drops and μ_N increases and as a result N-covered Ni(100) becomes the most stable termination. The optimum shape of the Ni nanoparticle exposes both the H-covered Ni(111) surface and the N-covered Ni(100) and (210) surfaces. This corresponds to the onset for surface nitridation. A further decrease of the H_2 partial pressure below 8×10^{-2} kPa results in a complete nitridation of the nanoparticle, and at a low H_2 pressure of 10^{-3} kPa (black hexagon in Figure 3), the $Ni_3N(101)$ surface presenting a N-excess becomes clearly the dominant facet. This Ni_3N phase is metastable in the sense that it would decompose extremely slowly into Ni and N_2 gas at 450 K[29], but fast at 700 K where decomposition is experimentally observed.[30] If both μ_N and μ_H are low (condition associated to the black triangle in Figure 3a), the bare Ni(111) surface becomes the most stable termination, and the Ni nanoparticle termination includes clean Ni(111), (110) and (221) surfaces and the N-covered Ni(100) surface (this surface would not be N-covered at μ_N lower than -9.2 eV). Overall, our simulations predict a key role of the H_2 pressure on the restructuration and phase transformation of Ni in the presence of NH_3. Noteworthy, a moderate H_2 partial pressure (10^{-2} times that of NH_3) appears to be sufficient on a (constrained) thermodynamic basis to avoid nitridation, as can be deduced by the frontier between the H/Ni(111) and N/Ni(100) domains on Figure 3b. In contrast, the formation of a metastable bulk nitride is only possible at low H_2 pressure (p_{H2} <10 Pa at p_{NH3} = 101 kPa and 350K).

To validate the theoretical stability diagrams in Figure 3, a series of temperature-programmed desorption experiments were conducted using unsupported Ni nanoparticles with an average size of *ca*. 80 nm (see SI for experimental details). After reduction under H_2, the Ni nanoparticles were submitted to a flow of either NH_3 or NH_3 + H_2 mixtures at 473 K for 3 h, as well as to a flow of NH_3 followed by H_2 for 3 h (Figure 4).

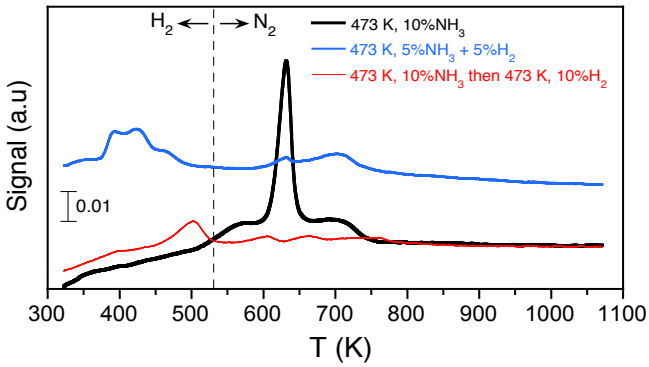

Figure 4. Temperature-programmed desorption profiles measured on unsupported metal Ni after treatment at 473 K for 3 h with 10%NH_3, 5%NH_3 + 5%H_2, and 10%NH_3 followed by hydrogenation at 473 K for 3 h. Experimental details, as well peak deconvolution and integration and thermal desorption profiles can be found in the SI (Table S5 and Figure S8).

The thermal profiles exhibited two characteristic gas desorption zones that can be assigned to H_2 (<573 K) and N_2 (>573 K).[31] Surface nitridation occurred upon exposure of the Ni nanoparticles to 10%NH_3 / 90%He at 473 K, resulting in the formation of an equivalent of 2.1 atomic layers of Ni_3N on the nanoparticles (Figure 4, black profile). When dosing 5%NH_3 / 5%H_2 / 90% He at 473 K concomitantly (Figure 4, blue profile) at N and H chemical potentials close to the black dot in Figure 3a, an equivalent of 0.24 atomic layers of Ni_3N were formed, which can be best described as a small coverage of chemisorbed N atoms on the Ni nanoparticles in agreement with the theoretical results. Dosing 10%H_2 / 90%He at 473 K after nitridation under 10%NH_3 / 90%He flow (Figure 4, red profile, Table S5) removed almost completely the nitride layer (presence of an equivalent of 0.58 atomic layers of Ni_3N). This body of results evidence the formation of surface nitride, (meta)stable until 700K, under NH_3 atmosphere, and its absence when H_2 is co-dosed in good agreement with the theoretical data.

The theoretical results reported above reflect that the formation of a N-covered Ni surface is a key driver for metal nitridation. To potentially extend our analysis to a broad range of metals, we can propose to use the N chemical potential at which N-adsorption becomes possible as a thermodynamic descriptor for onset nitridation and eventual deactivation. To this aim, fifteen transition metals were calculated: Co(fcc), Rh, Ir, Ni, Pd, Pt, Cu, Ag, Au, Ru, Re, Os, Fe, W, Mo. Figure 5a shows that the threshold μ_N at which the N-covered surface becomes more stable than the clean metal surface spans over 4 eV, reflecting a very different ability of each metal for stabilizing surface nitrides. Oxophilic metals at the left-hand side of the diagram (Mo, W, Fe) form N-covered structures at very low μ_N and are hence very prone to nitridation. In contrast, group 9 and 10 metals are more resistant to nitridation with a shift of ~1 or 2 eV to higher energy. The N-covered surface is stable against denitrification (forming N_2) at 450 K for the metals on the left of the $\mu_{0.5N2}$ arrow, while it is metastable for those on the right. Moreover, at the right-hand side of Figure 5a, Ag and Au can be regarded as inert against nitridation.

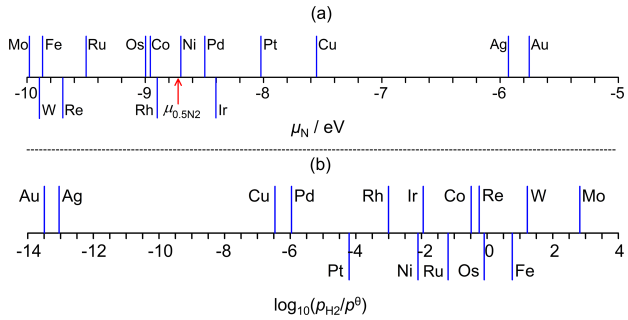

Figure 5. (a) Value of the nitrogen chemical potential (μ_N) where the nitrogen covered surface becomes more stable than the clean metal surface; (b) H_2 partial pressure where the hydrogen covered surface becomes more stable than the nitrogen covered surface at 450 K and p_{NH3} = 101 kPa. The red arrow indicates the chemical potential of ½ N_2 at 450 K.

The above stated surface nitridation trends are consistent with reported experimental findings. For example, the synthesis of noble metal nitrides is very challenging experimentally. For the synthesis of Pt, Ir and Pd nitrides (metals lying in the middle of our scale), extreme conditions

of 50 GPa / 2000 K, 48 GPa / 1600 K and 58 GPa / 1000 K at N_2 atmosphere, respectively, are required[7]. These results indicate that the synthesis of Pt nitride is more difficult than the synthesis of Ir and Pd nitrides, which is in agreement with the descriptor in Figure 5a. Cho *et al.*[17c,20d] also found a much faster deactivation of Co than Ni catalyst at the very same amination conditions, reflecting a lower nitridation tolerance for the former metal, in line with the position of Co at the left of Ni in Figure 5a. The position of Mo may seem surprising since the synthetic temperature of Mo_2N is higher than that of Ni_3N. Note that the value of the N chemical potential provides information on the stability of the nitride against the bare metal, but not of the oxide precursor used to generate Mo_2N. The high temperature required for the synthesis of Mo_2N is related to the conversion of MoO_3 into MoO_2 and Mo, a step that is kinetically controlled.[32]

The prevention of surface nitridation for catalysts by H_2 exposure requires understanding the competition between N- and H-adsorption. Figure 5b shows the threshold H_2 partial pressure needed, from a thermodynamic viewpoint, to avoid nitridation and hence potential deactivation of catalytic metals. The different interaction with H_2 somewhat changes the order between metals, making nitridation avoidance more difficult for Os, Co and Ir, and easier for Pd. Among amination catalysts Ru, Co and Os require a higher H_2 pressure than Ni to prevent deactivation. Experimentally, Ni was the first non-noble metal shown to be active for the amination of secondary alcohols with NH_3 and stable in the absence of H_2.[17] In contrast, Co deactivates in the absence of H_2 by nitride formation.[20d] From Figure 5, Cu is another interesting candidate, since it is even less prone to nitridation than Ni. The preparation of bimetallic catalysts such as CoNi and CoCu could be another route offering simultaneously a high activity and selectivity for alcohol amination to primary amines together with a good stability against nitridation in the absence of external H_2.

Turning round our viewpoint, one might be interested in metals forming surface nitrides that remain stable under a H_2 pressure. Mo, W and Fe meet this requirement according to Figure 5b, although this prediction should be certainly assessed using well-designed experiments. Although kinetic effects might modify quantitative values, such as the required H_2 pressure to prevent nitridation, the aforementioned trends derived from constrained thermodynamics should remain valid and general.

Conclusion

To sum up, our thermodynamic analysis shows that the interaction of nitrogen on Ni is termination specific. The dominant facet of a nanoparticle is modified depending on the experimental conditions: (111) surface for bare Ni, (100) for N-covered Ni and (101) for Ni_3N. This imposes a strong restructuration of the nanoparticle shape upon preferential adsorption of nitrogen in realistic gas phase conditions. The simulated trends for nitridation on a family of 15 transition metals exhibit contrasting situations. Nevertheless, surface nitride formation can be prevented in most cases by a moderate H_2 pressure. The formation of a H_2-resistant surface nitride only occurs for Mo, W and Fe. Hence key insights on the nitridation behavior of transition metals are provided which might give useful guidelines for the fine design of materials and catalysts.

Acknowledgements

This work was granted access to the HPC resources of CINES and IDRIS under the allocation 2015-080609 made by GENCI. It also benefited from the computational resources of the PSMN. Financial support was provided by the ANR grant SHAPES (13-CDII-0004-06).

Associated content: supporting Information available

Experimental and computational method details, calculated structures and energies, band deconvolution of figure 4, characterization of NiO sample are provided.

References

1 Oyama, S. T. *The Chemistry of Transition Metal Carbides and Nitrides*, Blackie Academic and Professional, Glasgow, **1996**.

2 Pierson, H. *Handbook of Refractory Carbides and Nitrides: Properties, Characteristics and Applications*, Noyes Publications, Westwood, NJ, **1996**.

3 Jhi, S. H.; Ihm, J.; Louie, S. G.; Cohen, M. L. *Nature* **1999**, *399*, 132-134.

4 a) Fry, A. *Stahl Eisen* **1923**, *43*, 1271-1279; b) Prenosil, B. *Härt.-Technol. Mitt.* **1973**, *28*, 157.

5 Gregoryanz, E.; Sanloup, C.; Somayazulu, M.; Badro, J.; Fiquet, G.; Mao, H. K.; Hemley, R. J. *Nat. Mater.* **2004**, *3*, 294-297.

6 Crowhurst, J. C.; Goncharov, A. F.; Sadigh, B.; Evans, C. L.; Morrall, P. G.; Ferreira, J. L.; Nelson, A. J. *Science* **2006**, *311*, 1275-1278.

7 Crowhurst, J. C.; Goncharov, A. F.; Sadigh, B.; Zaug, J. M.; Aberg, D.; Meng, Y.; Prakapenka, V. B. *J. Mater. Res.* **2008**, *23*, 1-5.

8 Young, A. F.; Sanloup, C.; Gregoryanz, E.; Scandolo, S.; Hemley, R. J.; Mao, H. K. *Phys. Rev. Lett.* **2006**, *96*, 155501.

9 Friedrich, A.; Winkler, B.; Bayarjargal, L.; Morgenroth, W.; Juarez-Arellano, E. A.; Milman, V.; Refson, K.; Kunz, M.; Chen, K. *Phys. Rev. Lett.* **2010**, *105*, 085504.

10 a) Kaner, R. B.; Gilman, J. J.; Tolbert, S. H. *Science* **2005**, *308*, 1268-1269; b) Cumberland, R. W.; Weinberger, M. B.; Gilman, J. J.; Clark, S. M.; Tolbert, S. H.; Kaner, R. B. *J. Am. Chem. Soc.* **2005**, *127*, 7264-7265.

11 McGee, R. C. V.; Bej, S. K.; Thompson, L. T. *Appl. Catal. A: Gen.* **2005**, *284*, 139-146.

12 Chen, W.-F.; Sasaki, K.; Ma, C.; Frenkel, A. I.; Marinkovic, N.; Muckerman, J. T.; Zhu, Y.; Adzic, R. R. *Angew. Chem. Int. Ed.* **2012**, *51*, 6131-6135.

13 a) Volpe, L.; Boudart, M. *J. Phys. Chem.* **1986**, *90*, 4874-4877; b) Kojima, R.; Aika, K. *Chem. Lett.* **2000**, *29*, 514-515; *c*) Boisen, A.; Dahl, S.; Jacobsen, C. J. H. *J. Catal.* **2002**, *208*, 180-186; d) Mckay, D.; Hargreaves, J. S. J.; Rico, J. L.; Rivera, J. L.; Sun, X. L. *J. Solid State Chem.* **2008**, *161*, 325-333; e) Hargreaves, J. S. J. *Appl. Petrochem. Res.* **2014**, *4*, 3-10.

14 Xu, K.; Chen, P.; Li, X.; Tong, Y.; Ding, H.; Wu, X.; Chu, W.; Peng, Z.; Wu, C.; Xie, Y. *J. Am. Chem. Soc.* **2015**, *137*, 4119-4125.

15 Borgna, A.; Fréty, R.; Primet, M.; Guénin, M. *Appl. Catal.* **1991**, *76*, 233-254.

16 a) Lawrence, S. A. *Amines: Synthesis, Properties and Applications*, Cambridge University Press, **2004**; b) Appoport, Z. *The Chemistry of Anilines*, John Wiley & Sons Ltd, **2007**; c) Pera-Titus, M.; Shi, F. *ChemSusChem.* **2014**, *7*, 1-4.

17 a) Shimizu, K-I.; Kon, K.; Onodera, W.; Yamazaki, H.; Kondo, J. N. *ACS Catal.* **2013**, *3*, 112-117; b) Shimizu, K-I.; Kon, K.; Onodera, W.;

Yamazaki, H.; Kondo, J. N. *ACS Catal*. **2013**, *3*, 998-1005; c) Cho, J. H.; Park, J. H.; Chang, T. S.; Kim, J. E.; Shin, C. H. *Catal. Lett.* **2013**, *143*, 1319-1327; d) Shimizu, K-I. *Catal. Sci. Technol.* **2015**, *5*, 1412-1427.

18 a) He, J.; Yamaguchi, K.; Mizuno, N. *Chem. Lett*. **2010**, *39*, 1182-1183; b) Dixit, M.; Mishra, M.; Joshi, P. A.; Shah, D. *Catal. Commun*. **2013**, *33*, 80-83; c) Santoro, F.; Psaro, R.; Ravasio, N.; Zaccheria, F. *ChemCatChem.* **2012**, *4*, 1249-1254.

19 a) Baiker, A.; Kijenski, J. *Catal. Rev. Sci. Eng*. **1985**, *27*, 653-697; b) Kimura, H.; Taniguchi, H. *Appl. Catal. A*: *Gen.* **2005**, *287*, 191-196; c) Imabeppu, M.; Kiyoga, K.; Okamura, S. ; Shoho, H.; Kimura, H. *Catal. Commun*. **2009**, *10*, 753-808; d) Li, Y.; Li, Q.; Zhi, L.; Zhang, M. *Catal. Lett*. **2011**, *141*, 1635-1642; e) Sun, J.; Jin, X.; Zhang, F. W.; Hu, W.; Liu, J.; Li, R. *Catal. Commun*. **2012**, *24*, 30-33.

20 a) Fischer, A.; Mallat, T.; Baiker, A. *J. Catal*. **1999**, *182*, 289-291; b) Jenzer, G.; Mallat, T.; Baiker, A. *Catal. Lett*. **1999**, *61*, 111-114; c) Imabeppu, M.; Kiyoga, K.; Okamura, S.; Shoho, H.; Kimura, H. *Catal. Commun*. **2009**, *10*, 753-808; d) Cho, J. H.; Park, J. H.; Chang, T. S.; Seo, G.; Shin, C. H. *Appl. Catal. A: Gen*. **2012**, *417-418*, 313-319.

21 Baiker, A. *The role of hydrogen in the catalytic amination of alcohols and the disproportionation of amines*, Guisnet, M.; Barrault, J. ; Bouchoule, C. ; Duprez, D. ; Montassier, C. ; Pérot, G. (Editors), Heterogeneous Catalysis and Fine Chemicals, Elsevier Science Publishers, Amsterdam, **1988**, pp 283-290.

22 Lee, J. H.; Hamrin Jr, C. E.; Davis, B. H. *Catal. Today* **1992**, *15*, 223-241.

23 a) Kresse, G.; Furthmüller, J. *Comput. Mater. Sci.* **1996**, *6*, 15-50; b) Kresse, G.; Furthmüller, J. *Phys. Rev. B* **1996**, *54*, 11169-11186.

24 a) Blochl, P. E. *Phys. Rev. B* **1994**, *50*, 17953; b) Kresse, G. *Phys. Rev. B* **1999**, *59*, 1758-1775.

25 Perdew, J. P.; Burke, K.; Ernzerhof, M. *Phys. Rev. Lett.* **1996**, *77*, 3865-3868.

26 Reuter, K.; Scheffler, M. *Phys. Rev. B* **2001**, *65*, 035406.

27 Duan, X. Z.; Qian, G.; Liu, Y.; Ji, J.; Zhou, X. G.; Chen, D.; Yuan, W. K. *Surf. Sci*. **2012**, *606*, 549-553.

28 Duan, X. Z.; Qian, G.; Fan, C.; Zhu, Y.; Zhou, X. G.; Chen, D.; Yuan, W. K. *Fuel Process. Technol*. **2013**, *108*, 112-117.

29 From our data, Ni_3N becomes less stable than 3Ni and $1/2N_2$ at T above room temperature in standard conditions.

30 Berndt, C. C.; Khor, K. A.; Lugscheider, E. F. *Thermal Spray 2001: New surfaces for a new millennium*, (ASM International, Material Park, Ohio, USA, **2001**).

31 a) Baiker, A.; Monti, D. *Ber. Bunsenges. Phys. Chem*. **1983**, *87*, 602-605; b) Al-Shammeri, K. K.; Saleh, J. M. *J. Chem. Phys*. **1986**, *90*, 2906-2910.

32 Cárdenas-Lizana, F.; Gómez-Quero, S.; Perret, N.; Kiwi-Minsker, L.; Keane, M. A. *Catal. Sci. Technol*. **2011**, *1*, 794-801.

TOC

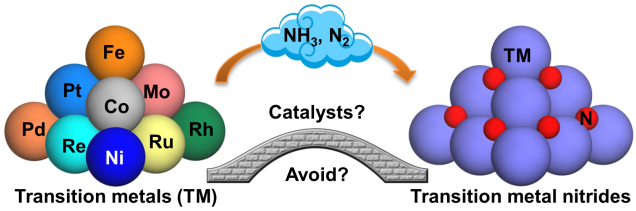
Fe
Pt
Mo
Co
Pd
Rh
Re
Ru
Ni
Transition metals (TM)
NH3, N2
Catalysts?
Avoid?
TM
N
Transition metal nitrides